ISSN 0915-633X

NATIONAL INSTITUTE FOR FUSION SCIENCE

Computational Study of Three Dimensional Equilibria with the Bootstrap Current

R. Kanno, N. Nakajima, T. Hayashi and M. Okamoto

(Received - Mar. 4, 1998)

NIFS-546 Mar. 1998

RESEARCH REPORT
NIFS Series

NAGOYA, JAPAN

Computational Study of Three Dimensional Equilibria with the Bootstrap Current

R. KANNO, N. NAKAJIMA, T. HAYASHI, and M. OKAMOTO
National Institute for Fusion Science, Toki 509-5292, Japan

Abstract
The three dimensional currentless equilibrium code, HINT, is revised so that it can handle equilibria with a net toroidal current, e.g. the bootstrap current. The revised HINT code is applied to equilibria of the Large Helical Device with good nested flux surfaces.

Keywords
HINT computation, 3D MHD equilibrium, stellarator, relaxation, bootstrap current

1. Introduction

To study three dimensional (3-D) MHD equilibria with a net toroidal current, the HINT code [1] is revised, which originally treats only currentless equilibria. The net toroidal current means such non-vanishing currents after the flux surface average as the bootstrap current, the Ohmic current, the Ohkawa current, etc. The calculation is based on the time dependent relaxation technique using small values of resistivity and viscosity. The original HINT code was applied to finite beta three dimensional equilibria without a net toroidal current, because three dimensional equilibria have the possibility of net current-free steady operation. Most important advantage of the HINT code is that it does not need to assume the existence of nested flux surfaces in equilibria. Thus, the HINT code enable us to investigate quantitatively 1) the deterioration of magnetic surfaces due to the magnetic island formation and 2) the self healing of magnetic islands in the finite beta plasma in three dimensional currentless equilibria (see Refs.[2, 3, 4]). Although the three dimensional equilibria have a possibility to exist under the currentless condition, net toroidal currents, namely, the bootstrap current and/or the Ohkawa current can flow according to the experimental conditions. The properties of the Large Helical Device (LHD) [5] equilibria with self consistent bootstrap current are examined [6, 7] and the effects of a net toroidal current on the Mercier stability are also investigated [8] under the assumption that nested good flux surfaces exist. The net toroidal current so drastically changes the rotational transform that the resonance condition of the magnetic island will be altered, which leads to the formation and/or self healing of magnetic islands. To investigate such phenomena, the HINT code has been revised. In this letter, we propose the revised HINT computational method and apply it to the LHD equilibria with good nested flux surfaces.

2. Modification of the HINT computation

In the HINT code, an MHD equilibrium is obtained starting from an arbitrary nonequilibrium initial plasma and vacuum field configuration by means of a time-dependent relaxation method with

small values of resistivity η and viscosity ν. Calculations are performed in the two steps, which have been first developed by Park et al. [9]. The first step (A-step) is the relaxation process of the pressure along magnetic field lines. To speed up the relaxation of the pressure, we solve the artificial sound wave equations under a fixed magnetic field, until $\boldsymbol{B} \cdot \nabla p = 0$ is satisfied, (see Refs.[1, 9]). This pressure relaxation scheme has been further developed by using a method where field lines are traced [2]. The newer scheme has been turned out to be more efficient when island chains appear on magnetic surfaces. The second step (B-step) is the relaxation process of the magnetic field under a fixed pressure profile, (see Refs.[1, 9]). To calculate the MHD equilibrium with a net toroidal current, we need to revise the Faraday's equation in the B-step, according to the following idea. In the original HINT code, the Faraday's equation is given as

$$\frac{\partial \boldsymbol{B}}{\partial t} = -\nabla \times \boldsymbol{E} = \nabla \times (\boldsymbol{v} \times \boldsymbol{B} - \eta \boldsymbol{j}). \quad (1)$$

In the steady state, $\boldsymbol{E}$ is expressed by the gradient of a scalar potential ϕ, i.e. $\boldsymbol{E} = -\nabla\phi$, in the Ohm's law given as

$$\boldsymbol{E} + \boldsymbol{v} \times \boldsymbol{B} = \eta \boldsymbol{j}. \quad (2)$$

If there exist closed flux surfaces, calculation of a flux surface average is permitted on such surfaces. For some equilibria without a source of a net current, the scalar potential become a single-valued function, so that

$$\langle \boldsymbol{E} \cdot \boldsymbol{B} \rangle = -\langle \nabla\phi \cdot \boldsymbol{B} \rangle = 0 = \eta \langle \boldsymbol{j} \cdot \boldsymbol{B} \rangle, \quad (3)$$

where $\langle\ \rangle$ means the flux surface average. Thus, we obtain three dimensional equilibria without a net current (see Ref.[9]).

For equilibria with an Ohmic current, the Ohm's law given by Eq.(2) can be represented as follows;

$$\boldsymbol{E} + \boldsymbol{v} \times \boldsymbol{B} = \eta (\boldsymbol{j} - \sigma \boldsymbol{E}_{\rm ex}), \quad (4)$$

where σ is the conductivity and $\sigma \boldsymbol{E}_{\rm ex}$ is the Ohmic current. Since the Ohmic current can be also represented as $\boldsymbol{B} \langle \boldsymbol{j} \cdot \boldsymbol{B} \rangle_{\rm Ohmic} / \langle B^2 \rangle$, the revised equation of Eq.(1) becomes

$$\frac{\partial \boldsymbol{B}}{\partial t} = \nabla \times \left(\boldsymbol{v} \times \boldsymbol{B} - \eta \left\{ \boldsymbol{j} - \boldsymbol{B} \frac{\langle \boldsymbol{j} \cdot \boldsymbol{B} \rangle_{\rm Ohmic}}{\langle B^2 \rangle} \right\} \right), \quad (5)$$

where we assume that an equilibrium has closed flux surfaces. If there exist closed flux surfaces in the steady state, we have

$$\langle \boldsymbol{E} \cdot \boldsymbol{B} \rangle = 0 = \eta \{ \langle \boldsymbol{j} \cdot \boldsymbol{B} \rangle - \langle \boldsymbol{j} \cdot \boldsymbol{B} \rangle_{\rm Ohmic} \}. \quad (6)$$

Thus, in the steady state $\langle \boldsymbol{j} \cdot \boldsymbol{B} \rangle$ becomes $\langle \boldsymbol{j} \cdot \boldsymbol{B} \rangle_{\rm Ohmic}$, and we obtain three dimensional equilibria with the net Ohmic current. If there are also the bootstrap current and the Ohkawa current, Eq.(5) can be generalized as

$$\frac{\partial \boldsymbol{B}}{\partial t} = \nabla \times \left(\boldsymbol{v} \times \boldsymbol{B} - \eta \left\{ \boldsymbol{j} - \boldsymbol{B} \frac{\langle \boldsymbol{j} \cdot \boldsymbol{B} \rangle_{\rm net}}{\langle B^2 \rangle} \right\} \right), \quad (7)$$

where

$$\langle \boldsymbol{j} \cdot \boldsymbol{B} \rangle_{\rm net} = \langle \boldsymbol{j} \cdot \boldsymbol{B} \rangle_{\rm Ohmic} + \langle \boldsymbol{j} \cdot \boldsymbol{B} \rangle_{\rm bootstrap} + \langle \boldsymbol{j} \cdot \boldsymbol{B} \rangle_{\rm Ohkawa}. \quad (8)$$

Therefore, we treat Eq.(7) in the revised B-step, instead of Eq.(1). Solving numerically the relaxation equations in the revised HINT computational method, we find a 3-D MHD equilibrium with a net current in a toroidal helical system.

Calculation of a net toroidal current, e.g. the bootstrap current, is done between the A and B steps under conditions of a fixed pressure profile and a fixed magnetic field with closed flux surfaces. In the calculation of the bootstrap current, we employed the Boozer coordinates (ψ, θ, ζ), where ψ is the toroidal magnetic flux, and θ and ζ are the poloidal and toroidal angles, respectively. The bootstrap current is expressed in each collisionality limits as follows;

$$\langle \boldsymbol{j} \cdot \boldsymbol{B} \rangle_{\rm bootstrap} = -G_{\rm bs} \left(L_1 \frac{{\rm d}p}{{\rm d}\psi} + L_2 n \frac{{\rm d}T}{{\rm d}\psi} \right), \quad (9)$$

where p is the plasma pressure, n is the density, T is the temperature ($p = 2nT$: $n = n_i = n_e$, $T = T_i = T_e$, and $n, T \propto \sqrt{p}$ in this work). L_1 and L_2 are transport coefficients, which are composed of the viscosity and the friction coefficients, and G_{bs} is a geometrical factor given in Refs.[6, 7, 8, 10]. To evaluate the bootstrap current through Eq.(9), only spectra of the magnetic field strength in the Boozer coordinates are needed with some surface quantities (see Refs.[6, 7, 8, 10]). To obtain the spectra of the magnetic field strength and surface quantities, we use the method in Refs.[11, 12] with the magnetic field line trace. To estimate the bootstrap current in various collisionality regimes, we use the connection formula derived in Ref.[8], instead of Eq.(9).

3. Application of the revised HINT code

We apply the revised HINT code to the LHD equilibrium with the bootstrap current. We consider the equilibrium with $B_0 = 4$ T, $R_0 = 4$ m, $\beta_0 = 1.4$ %, $n_0 = 7.5 \times 10^{19}$ m^{-3}, and $T_0 = 4$ keV at the magnetic axis. Here, in this calculation the equilibrium has the structure of good nested flux surfaces. In this case, the amount of the bootstrap current, I_{net}, is about 50 kA, where I_{net} is defined as

$$I_{net} \equiv \int \mathrm{d}\boldsymbol{S}_T \cdot \boldsymbol{j}_{net}, \qquad (10)$$

$\boldsymbol{S}_T$ is the poloidal cross section, and $\boldsymbol{j}_{net} = \boldsymbol{B} \langle \boldsymbol{j} \cdot \boldsymbol{B} \rangle_{net} / \langle B^2 \rangle$. Poincare plots of field lines, profiles of the pressure and the toroidal current, and the rotational transform are shown in Fig.1. To evaluate the bootstrap current, Fourier spectra of the magnetic field strength in the Boozer coordinates are calculated as in Fig.2, according to the method in Refs.[11, 12]. As shown in Fig.3, the profile of the bootstrap current is obtained by using the Fourier spectra. The profile of the bootstrap current can be explained by using the geometrical factor G_{bs}, the pressure gradient $\mathrm{d}p/\mathrm{d}\psi$, and the temperature gradient $\mathrm{d}T/\mathrm{d}\psi$ (see Eq.(9)). In this calculation, the plasma is in the collisionless regime except for near the magnetic axis, as shown in Fig.4, and the behavior of the geometrical factor is dominated by one for the $1/\nu$ regime (see Fig.5). Gradients of the pressure and temperature become zero at the outermost surface. These behaviors are reflected in the profile of the bootstrap current. Adding the bootstrap current shown in Fig.3 on the Pfirsch-Schlüter current, the current profile is modified from Fig.1b-1 to Fig.1b-2, and the rotational transform ι is increased as shown in Fig.1c-2 (compare to Fig.1c-1).

The error of force balance R_f in the above calculation is less than 10^{-5}, thus the new computational method is correctly working, where R_f is defined as

$$R_f = \frac{\int \mathrm{d}\tau \left(\nabla p - \boldsymbol{j} \times \boldsymbol{B}\right)^2}{\int \mathrm{d}\tau \left\{(\nabla p)^2 + (\boldsymbol{j} \times \boldsymbol{B})^2\right\}}. \qquad (11)$$

4. Conclusions

We have revised the HINT code, to study 3-D MHD equilibria with the bootstrap current. To develop the original HINT code, we have proposed the modification of the Faraday's equation in the scheme in the original HINT computation. The bootstrap current is calculated by using the method in Refs.[11, 12]. The revised HINT code is applied to the LHD equilibrium, and the validity of the code is ascertained.

Effects of a net current, especially the bootstrap current, on magnetic islands are under investigation. We are going to develop the revised HINT code to calculate equilibria with island chains.

References

[1] HAYASHI, T., Theory of Fusion Plasmas (CRPP Association EURATOM, Lausanne, 1989), pp.11.; HARAFUJI, K., HAYASHI, T., SATO, T., J. Comput. Phys. **81** (1989) 169.

[2] HAYASHI, T., TAKEI, A., SATO, T., Phys. Fluids B **4** (1992) 1539.

[3] HAYASHI, T., SATO, T., MERKEL, P., NÜHRENBERG, J., SCHWENN, U., Phys. Plasmas **1** (1994) 3262.

[4] HAYASHI, T., SATO, T., GARDNER, H.J., MEISS, J.D., Phys. Plasmas **2** (1995) 752.

[5] IIYOSHI, A., FUJIWARA, M., MOTOJIMA, O., OYABU, N., and YAMAZAKI, K., Fusion Technol. **17** (1990) 169.

[6] NAKAJIMA, N., OKAMOTO, M., J. Phys. Soc. Jpn. **61** (1992) 833.

[7] WATANABE, K., NAKAJIMA, N., OKAMOTO, M., NAKAMURA, Y., WAKATANI, M., Nucl. Fusion **32** (1992) 1499.

[8] WATANABE, K.Y., NAKAJIMA, N., OKAMOTO, M., YAMAZAKI, K., NAKAMURA,Y., WAKATANI,M., Nucl. Fusion **35** (1995) 335.

[9] PARK, W., MONTICELLO, D.A., STRAUSS, H., MANICKAM, J., Phys. Fluids **29** (1986) 1171.

[10] ICHIGUCHI, K., NAKAJIMA, N., OKAMOTO, M., Nucl. Fusion **37** (1997) 1109.

[11] BOOZER, A.H., Phys. Fluids **25** (1982) 520.

[12] ROME, J.A., J. Comput. Phys. **82** (1989) 348.

Figure Captions

Fig.1: The LHD equilibrium for the case of $\beta_0 = 1.4$ %; a) Poincare plots of field lines at the vertically elongated poloidal cross section, b) the current profile at the vertically elongated poloidal cross section, c) the profile of the rotational transform $|\iota|$. Figures a,b,c-1) show results for the currentless LHD, and a,b,c-2) are results for the LHD with the bootstrap current.

Fig.2: Fourier components of the magnetic field strength as a function of $\sqrt{\psi/\psi_{\rm edge}}$. In this figure, we show the largest seven components used in the calculation of the bootstrap current, except for $B_{0,0}$.

Fig.3: Profiles of the bootstrap current $\langle j \cdot B \rangle_{\rm bs} / \langle B^2 \rangle$ and the pressure as a function of $\sqrt{\psi/\psi_{\rm edge}}$.

Fig.4: The collision frequency normalized by the bounce frequency ω_b.

Fig.5: Geometrical factors for the $1/\nu$, the plateau (pl), and the Pfirsch-Schlüter (PS) regimes.

Fig.1

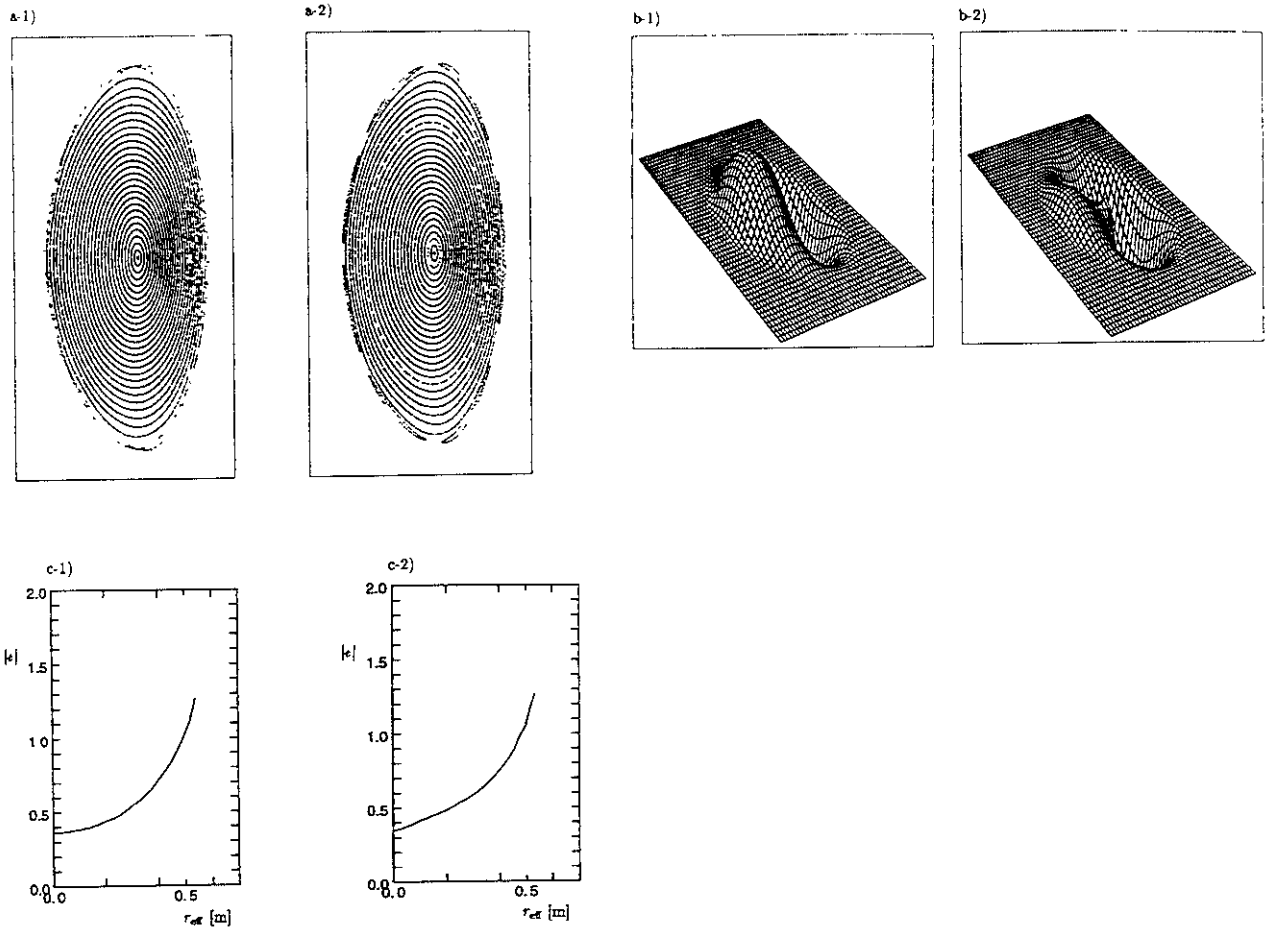
a-1)
a-2)
b-1)
b-2)
c-1)
c-2)
|ε|
2.0
1.5
1.0
0.5
0.0
0.0
0.5
r_{eff} [m]

Fig.2

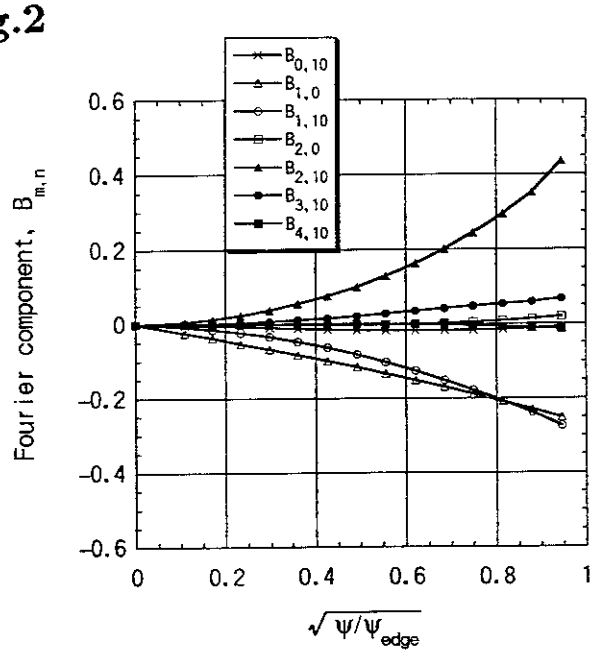
$B_{0,10}$
$B_{1,0}$
$B_{1,10}$
$B_{2,0}$
$B_{2,10}$
$B_{3,10}$
$B_{4,10}$
Fourier component, $B_{m,n}$
0.6
0.4
0.2
0
-0.2
-0.4
-0.6
0
0.2
0.4
0.6
0.8
1
$\sqrt{\psi/\psi_{edge}}$

Fig.3

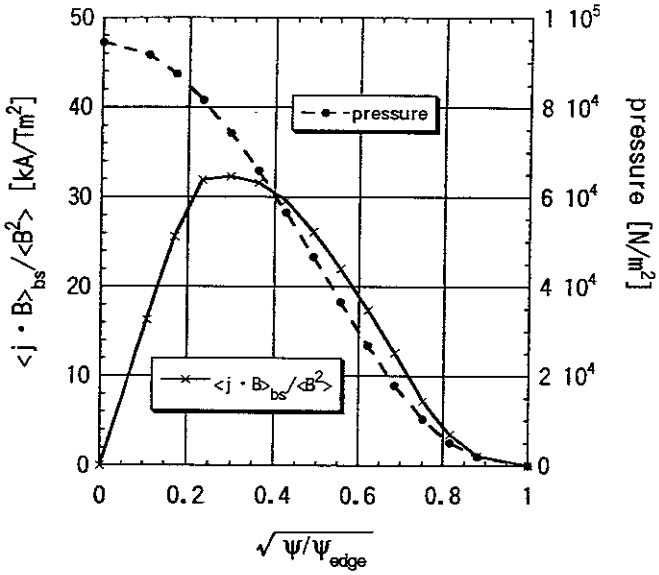

Fig.4

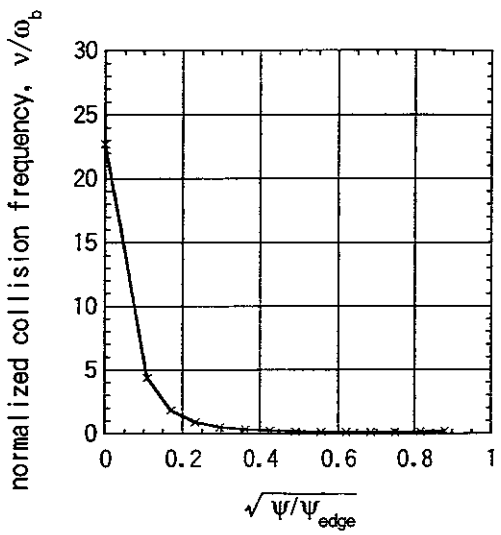

Fig.5

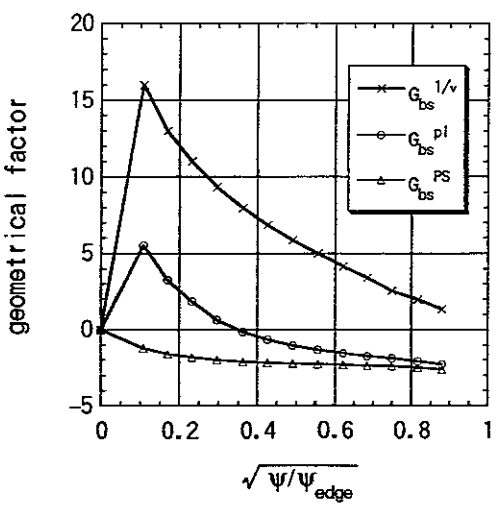

Recent Issues of NIFS Series

NIFS-510 C.C Hegna and N Nakajima,
On the Stability of Mercier and Ballooning Modes in Stellarator Configurations; Oct. 1997

NIFS-511 K Orito and T. Hatori,
Rotation and Oscillation of Nonlinear Dipole Vortex in the Drift-Unstable Plasma; Oct. 1997

NIFS-512 J. Uramoto,
Clear Detection of Negative Pionlike Particles from H_2 Gas Discharge in Magnetic Field; Oct. 1997

NIFS-513 T Shimozuma, M. Sato, Y. Takita, S. Ito, S Kubo, H Idei, K Ohkubo, T. Watari, T.S. Chu, K. Felch, P. Cahalan and C.M. Loring, Jr,
The First Preliminary Experiments on an 84 GHz Gyrotron with a Single-Stage Depressed Collector; Oct 1997

NIFS-514 T. Shimozuma, S. Monmoto, M. Sato, Y. Takita, S. Ito, S. Kubo, H. Idei, K. Ohkubo and T. Watari,
A Forced Gas-Cooled Single-Disk Window Using Silicon Nitride Composite for High Power CW Millimeter Waves; Oct 1997

NIFS-515 K. Akaishi,
On the Solution of the Outgassing Equation for the Pump-down of an Unbaked Vacuum System; Oct. 1997

NIFS-516 *Papers Presented at the 6th H-mode Workshop (Seeon, Germany)*; Oct. 1997

NIFS-517 John L Johnson,
The Quest for Fusion Energy; Oct. 1997

NIFS-518 J Chen, N. Nakajima and M. Okamoto,
Shift-and-Inverse Lanczos Algorithm for Ideal MHD Stability Analysis; Nov 1997

NIFS-519 M. Yokoyama, N Nakajima and M. Okamoto,
Nonlinear Incompressible Poloidal Viscosity in L=2 Heliotron and Quasi-Symmetric Stellarators; Nov. 1997

NIFS-520 S. Kida and H. Miura,
Identificaiton and Analysis of Vortical Structures; Nov 1997

NIFS-521 K Ida, S. Nishimura, T Minami, K. Tanaka, S. Okamura, M Osakabe, H. Idei, S. Kubo, C. Takahashi and K. Matsuoka,
High Ion Temperature Mode in CHS Heliotron/torsatron Plasmas, Nov. 1997

NIFS-522 M. Yokoyama, N Nakajima and M. Okamoto,
Realization and Classification of Symmetric Stellarator Configurations through Plasma Boundary Modulations; Dec. 1997

NIFS-523 H. Kitauchi,
Topological Structure of Magnetic Flux Lines Generated by Thermal Convection in a Rotating Spherical Shell; Dec. 1997

NIFS-524 T. Ohkawa,
Tunneling Electron Trap; Dec. 1997

NIFS-525 K. Itoh, S.-I. Itoh, M. Yagi, A. Fukuyama,
Solitary Radial Electric Field Structure in Tokamak Plasmas, Dec. 1997

NIFS-526 Andrey N. Lyakhov,
Alfven Instabilities in FRC Plasma; Dec 1997

NIFS-527 J. Uramoto,
Net Current Increment of negative Muonlike Particle Produced by the Electron and Positive Ion Bunch-method; Dec. 1997

NIFS-528 Andrey N. Lyakhov,
Comments on Electrostastic Drift Instabilities in Field Reversed Configuraiton; Dec. 1997

NIFS-529 J. Uramoto,
Pair Creation of Negative and Positive Pionlike (Muonlike) Particle by Interaction between an Electron Bunch and a Positive Ion Bunch; Dec. 1997

NIFS-530 J. Uramoto,
Measuring Method of Decay Time of Negative Muonlike Particle by Beam Collector Applied RF Bias Voltage; Dec. 1997

NIFS-531 J. Uramoto,
Confirmation Method for Metal Plate Penetration of Low Energy Negative Pionlike or Muonlike Particle Beam under Positive Ions; Dec. 1997

NIFS-532 J. Uramoto,
Pair Creations of Negative and Positive Pionlike (Muonlike) Particle or K Mesonlike (Muonlike) Particle in H2 or D2 Gas Discharge in Magnetic Field; Dec. 1997

NIFS-533 S. Kawata, C. Boonmee, T. Teramoto, L. Drska, J. Limpouch, R. Liska, M. Sinor,
Computer-Assisted Particle-in-Cell Code Development; Dec. 1997

NIFS-534 Y. Matsukawa, T. Suda, S. Ohnuki and C. Namba,
Microstructure and Mechanical Property of Neutron Irradiated TiNi Shape Memory Alloy; Jan. 1998

NIFS-535 A. Fujisawa, H. Iguchi, H. Idei, S. Kubo, K. Matsuoka, S. Okamura, K. Tanaka, T. Minami, S. Ohdachi, S. Morita, H. Zushi, S. Lee, M. Osakabe, R. Akiyama, Y. Yoshimura, K. Toi, H. Sanuki, K. Itoh, A. Shimizu, S. Takagi, A. Ejiri, C. Takahashi, M. Kojima, S Hidekuma, K. Ida, S. Nishimura, N. Inoue, R. Sakamoto, S.-I. Itoh, Y. Hamada, M. Fujiwara,
Discovery of Electric Pulsation in a Toroidal Helical Plasma; Jan. 1998

NIFS-536 Lj.R. Hadzievski, M.M. Skoric, M. Kono and T Sato,
Simulation of Weak and Strong Langmuir Collapse Regimes; Jan. 1998

NIFS-537 H. Sugama, W. Horton,
Nonlinear Electromagnetic Gyrokinetic Equation for Plasmas with Large Mean Flows; Feb. 1998

NIFS-538 H. Iguchi, T.P. Crowley, A. Fujisawa, S. Lee, K. Tanaka, T. Minami, S. Nishimura, K. Ida, R. Akiyama, Y. Hamada, H., Idei. M. Isobe, M. Kojima, S. Kubo, S. Morita, S. Ohdachi, S. Okamura, M. Osakabe, K. Matsuoka, C. Takahashi and K. Toi,
Space Potential Fluctuations during MHD Activities in the Compact Helical System (CHS); Feb. 1998

NIFS-539 Takashi Yabe and Yan Zhang,
Effect of Ambient Gas on Three-Dimensional Breakup in Coronet Formation Process; Feb. 1998

NIFS-540 H. Nakamura, K. Ikeda and S. Yamaguchi,
Transport Coefficients of InSb in a Strong Magnetic Field; Feb. 1998

NIFS-541 J. Uramoto,
Development of ν_μ Beam Detector and Large Area ν_μ Beam Source by H_2 Gas Discharge (I); Mar. 1998

NIFS-542 J. Uramoto,
Development of $bar\{\nu\}_\mu$ Beam Detector and Large Area $bar\{\nu\}_\mu$ Beam Source by H_2 Gas Discharge (II); Mar. 1998

NIFS-543 J. Uramoto,
Some Problems inside a Mass Analyzer for Pions Extracted from a H_2 Gas Discharge; Mar. 1998

NIFS-544 J. Uramoto,
Simplified ν_μ $bar\{\nu\}_\mu$ Beam Detector and ν_μ $bar\{\nu\}_\mu$ Beam Source by Interaction between an Electron Bunch and a Positive Ion Bunch; Mar. 1998

NIFS-545 J. Uramoto,
Various Neutrino Beams Generated by D_2 Gas Discharge; Mar.1998

NIFS-546 R. Kanno, N. Nakajima, T. Hayashi and M. Okamoto,
Computational Study of Three Dimensional Equilibria with the Bootstrap Current; Mar. 1998